Biointerface Research in Applied Chemistry
Open-Access Journal (ISSN: 2069-5837)

Article
Volume 15, Issue 4, 2025, 52
https://doi.org/10.33263/BRIAC154.052

Modified Cyclic Tetra-Amino Acid-based Compounds-Potential Human Insulin Degrading Enzyme Inhibitors: Insilico Approach

Cecilia O. Akintayo [1*], Abel Kolawole Oyebamiji [2,3,*], Arogundade Ibukun O [1], Adeniyi Adebayo [1], Sunday Adewale Akintelu [4], Samson Olusegun Afolabi [5]

[1] Chemistry Department, Federal University Oye Ekiti, Ekiti State, Nigeria; cecilia.akintayo@fuoye.edu.ng (C.O.A);
[2] Department of Industrial Chemistry, University of Ilesa, Ilesa, Osun State, Nigeria; abel_oyebamiji@unilesa.edu.ng (A.K.O.);
[3] Good Health and Wellbeing Research Clusters (SDG 03), University of Ilesa, Ilesa, Osun State, Nigeria;
[4] School of Chemistry and Physics, University of KwaZulu-Natal, Durban, South Africa. akintelus@ukzn.ac.za (S.A.A);
[5] Infochemistry Scientific Center, ITMO University, Saint Petersburg 191002, Russia; olusegunafolabi2@itmo.ru;
* Correspondence: abel_oyebamiji@unilesa.edu.ng; and cecilia.akintayo@fuoye.edu.ng

Received: 31.01.2025; Accepted: 24.07.2025; Published: 9.05.2025

Abstract: We examined the effect of electron-withdrawing and donating groups on the biochemical activity of modified cyclic tetra-amino acid-based compounds as human insulin-degrading enzyme inhibitors and predicted a library of drug-like compounds with potent cytotoxicity using an in silico approach. The chosen compounds underwent docking and absorption, distribution, metabolism, excretion, and toxicity (ADMET) analyses after being optimized. We found that the hydrogen bond strength between the modified cyclic tetra-amino acid-based compounds and ARG 765 and ASN841, which are positioned in the binding site of the human insulin-degrading enzyme (2g56), was significantly increased upon the addition of propionamide. Also, mutual coordination of methyl (3S,9S,12S)-9-(3-amino-3-oxopropyl)-12-(5-chloro-1,3-dioxoisoindolin-2-yl)-5,8,11-trioxo-4,7,10-triaza-1(1,3)-benzenacyclotridecaphane-3-carboxylate and human insulin-degrading enzyme (2g56) showed enhanced binding propensity with a calculated binding affinity value of -7.96747208 kcal mol-1, compared to other studied molecules. As possible anti-human insulin-degrading enzyme agents, this work may help design and construct a library of effective modified cyclic tetra-amino acid-based compounds.

Keywords: peptides; inhibitors; *insilico*; diabetes.

1. Introduction

Diabetes mellitus has been reported to affect millions of people worldwide [1, 2]. It is considered one of the major challenges facing the medical community, and the urgent need to find a lasting solution has attracted significant attention from researchers [3, 4]. In many cases, diabetes mellitus goes undiagnosed, presenting complications related to the body's primary glycemic regulator [5]. The metabolic abnormalities associated with diabetes mellitus lead to secondary pathophysiological changes in various organ systems, placing a significant burden on both patients and healthcare systems [6]. According to several studies, numerous efforts

have been made to control diabetes mellitus using conventional therapies; however, these approaches have faced several limitations [7, 8]. Moreover, the adverse effects linked to many approved drugs have driven ongoing efforts to design and develop more effective drug-like agents with minimal or no toxicity and side effects [9].

Insulin-degrading enzyme (IDE) is a large zinc-binding protease belonging to the M16 metalloprotease family, and it is widely recognized for its ability to degrade a variety of short, amino acid–based peptides with diverse structures [10]. This neutral Zn^2-dependent metalloendopeptidase is expressed in both insulin-responsive and non-responsive cells [11]. Several studies have reported that IDE can associate with cellular membranes; however, the exact nature of its membrane interaction remains undefined. As a result, IDE has become a focus of intense research, particularly as a potential target for modulating diabetes-related pathways in humans [12, 13].

Peptides are short chains of amino acids linked by peptide bonds [14]. These molecules have been reported as promising therapeutic agents with diverse applications, including anticancer and antimalarial treatments [15]. According to several studies, peptide derivatives exhibit enhanced specificity and selectivity, enabling them to combat various diseases effectively [16–18]. Cyclic peptides, in particular, have been successfully synthesized by many researchers using automated techniques. Their therapeutic potential has attracted significant scientific interest, leading to ongoing investigations into their biological activities [19, 20]. Research has demonstrated that cyclic peptides have the potential to function as drug-like agents due to key properties such as low toxicity, high specificity and selectivity, and favorable binding characteristics [21]. As a result, cyclic peptides have become important target molecules in the design of novel, efficient therapeutics. According to Chakraborty *et al*. [22], cyclic peptides possess constrained conformations, which have been reported to enhance metabolic stability, target affinity, and selectivity [23]. In this study, the incorporation of electron-withdrawing and electron-donating groups is expected to improve human metabolic stability and promote better target recognition and binding. Therefore, this study was conducted to evaluate the effectiveness of the modified compounds as inhibitors of the human insulin-degrading enzyme.

2. Materials and Methods

2.1. Density functional theory-based optimization.

The modeled compounds were optimized at the density functional theory with the standard 6-31+G* basis set. In the method employed in this work (density functional theory), three-feature B3LYP was utilized, and this consists of Becke's gradient exchange correction [24] and the Lee, Yang, Parr correlation functional [25]. The time frame for the minimization of the studied compounds was due to the size of the selected individual molecule and the descriptors generated after the calculations were reported (Table 1). More so, the choice of these compounds was due to the high selectivity, efficacy, and favorable toxicity profile compared to small molecules. Also, the optimized ligands were further subjected to other software for further studies.

Table 1. Studied phytochemicals of modified cyclic tetra-amino acid-based compounds.

	Structure	IUPAC
1	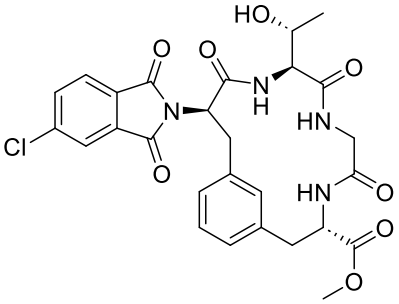	methyl (3S,9S,12R)-12-(5-chloro-1,3-dioxoisoindolin-2-yl)-9-((R)-1-hydroxyethyl)-5,8,11-trioxo-4,7,10-triaza-1(1,3)-benzenacyclotridecaphane-3-carboxylate
2	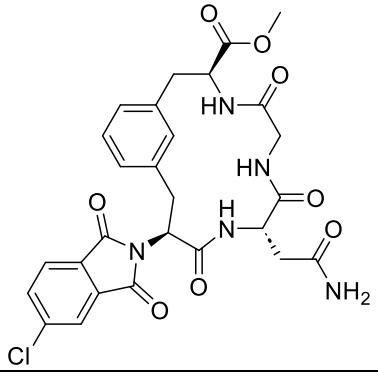	methyl (3S,9S,12S)-9-(2-amino-2-oxoethyl)-12-(5-chloro-1,3-dioxoisoindolin-2-yl)-5,8,11-trioxo-4,7,10-triaza-1(1,3)-benzenacyclotridecaphane-3-carboxylate
3	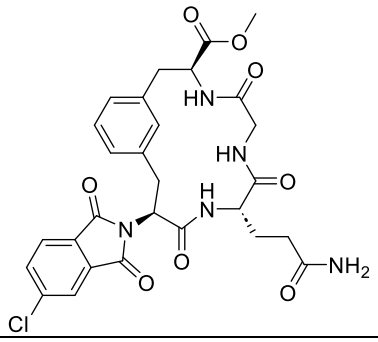	methyl (3S,9S,12S)-9-(3-amino-3-oxopropyl)-12-(5-chloro-1,3-dioxoisoindolin-2-yl)-5,8,11-trioxo-4,7,10-triaza-1(1,3)-benzenacyclotridecaphane-3-carboxylate
4	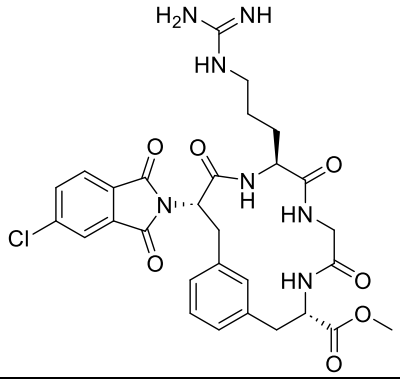	methyl (3S,9S,12S)-12-(5-chloro-1,3-dioxoisoindolin-2-yl)-9-(3-guanidinopropyl)-5,8,11-trioxo-4,7,10-triaza-1(1,3)-benzenacyclotridecaphane-3-carboxylate
5	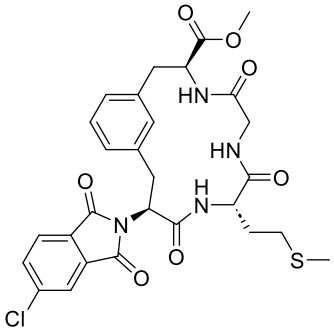	methyl (3S,9S,12S)-12-(5-chloro-1,3-dioxoisoindolin-2-yl)-9-(2-(methylthio)ethyl)-5,8,11-trioxo-4,7,10-triaza-1(1,3)-benzenacyclotridecaphane-3-carboxylate

	Structure	IUPAC
6	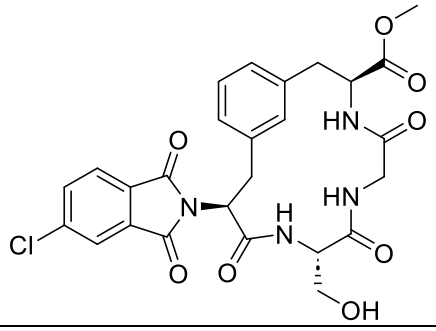	methyl (3S,9S,12S)-12-(5-chloro-1,3-dioxoisoindolin-2-yl)-9-(hydroxymethyl)-5,8,11-trioxo-4,7,10-triaza-1(1,3)-benzenacyclotridecaphane-3-carboxylate
7	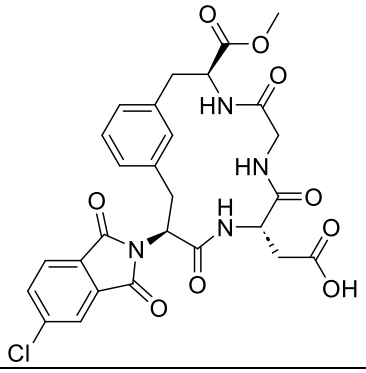	2-((3S,9S,12S)-12-(5-chloro-1,3-dioxoisoindolin-2-yl)-3-(methoxycarbonyl)-5,8,11-trioxo-4,7,10-triaza-1(1,3)-benzenacyclotridecaphane-9-yl)acetic acid
8	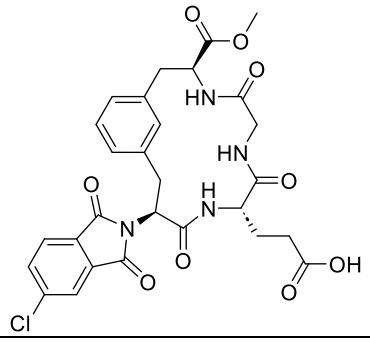	3-((3S,9S,12S)-12-(5-chloro-1,3-dioxoisoindolin-2-yl)-3-(methoxycarbonyl)-5,8,11-trioxo-4,7,10-triaza-1(1,3)-benzenacyclotridecaphane-9-yl)propanoic acid
9	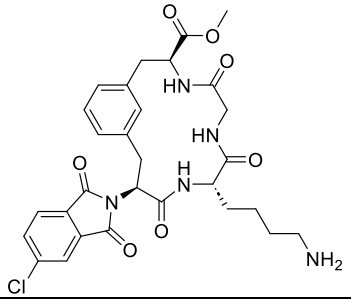	methyl (3S,9S,12S)-9-(4-aminobutyl)-12-(5-chloro-1,3-dioxoisoindolin-2-yl)-5,8,11-trioxo-4,7,10-triaza-1(1,3)-benzenacyclotridecaphane-3-carboxylate
10	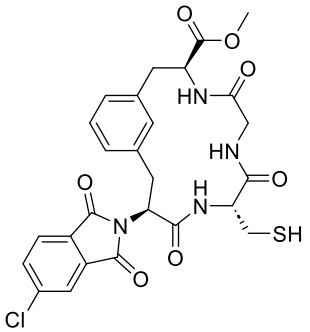	methyl (3S,9R,12S)-12-(5-chloro-1,3-dioxoisoindolin-2-yl)-9-(mercaptomethyl)-5,8,11-trioxo-4,7,10-triaza-1(1,3)-benzenacyclotridecaphane-3-carboxylate

Note: tables are original and non-published or taken from open-access sources

2.2. Induce fit molecular docking analysis.

Human insulin-degrading enzyme with protein data bank identification number (2g56) [26] was obtained from the protein database (https://www.rcsb.org/structure/2G56). The

downloaded human insulin-degrading enzyme was cleaned and prepared for induced fit docking calculation using molecular operating environment software (MOE) [27] which includes (i) removal of water and ligand molecules which were irrelevant to molecular docking calculation; (ii) addition of hydrogen atoms to the studied receptor and this was due to their significant roles in interaction with studied molecules; (iii) Allocating suitable charges and (iv) and minimizing the structure (for example, by employing energy reduction to alleviate steric conflicts) and fixing any structural problems (such as missing residues or chains).

Also, the studied ligands were prepared using a similar method to the preparation of the studied receptor. The 2 and 3-dimensional structures of the studied compounds were modeled using ChemDraw 22.2.0 version [28] and Spartan 14 software [29]. Appropriate hydrogen atoms/charges were added to the 3-dimensional structure of the studied ligand, and the modeled studied compounds were minimized to acquire a steady conformation.

2.3. Molecular dynamic simulation of lead compound.

Ubuntu was used to execute molecular dynamic simulations using the GROMACS 2202.2 [30] package as well as the CGenFF force field [31]. To retrieve the receptors for the topology, the pdb2gmx command was utilized. Https://www.swissparam.ch server was used to parameterize the studied ligands [32]. A water model (TIP3P) with a dodecahedron box configuration and a distance of 1 nm from the protein edges in all directions was used to solvate all systems. To imitate a physiological buffer solution, 0.15 M of NaCl was added, and Na+ and Cl-ions were added to neutralize the system.

Moreover, F_{max} was kept below 1000 kJ/mol nm using a 500-step steep descent approach to reduce energy and get rid of any steric collisions and undesired interactions. The NVT and NPT systems were then balanced, with a modified Berendsen thermostat and a Berendsen barostat used to maintain a temperature of 300 K for 100 ps and a constant pressure at 1 bar level. Each of the two complexes underwent 100 ns of molecular dynamics modeling utilizing particle-mesh Ewald electrostatics with stable temperature and pressure, a time step of 2 fs, and a long-range interaction limit of 1 nm [33]. Trajectories were shown using Pymol and analyzed using a variety of GROMACS scripts.

2.4. Molecular mechanics/Poisson-Boltzmann surface area (MM-PBSA).

The Molecular Mechanics/Poisson-Boltzmann Surface Area (MM-PBSA) approach, as described by Kumari *et al*. in 2014 [34], is a technique for assessing the binding affinity of an inhibitor protein. Generally, the free binding energy of protein-ligand complexes can be computed using g_mmpbsa in conjunction with molecular dynamics (MD) modeling (Equation 1). Also, using equations 2 and 3, free energies and free solvation energies can be calculated.

$$\Delta G_{binding} = \Delta G_{complex} - \left(\Delta G_{protein} + \Delta G_{ligand}\right) \quad (1)$$

$$\Delta G = E_{MM} + G_{solvation} \quad (2)$$

$$\Delta G_{solvation} = \Delta G_{polar} + \Delta G_{nonpolar} \quad (3)$$

2.5. ADMET Examination for lead ligand and reference ligand.

The ADMET characteristic of the lead compound was predicted using the freely accessible SwissADME software [35]. Key molecular parameters, including molecular weight,

the count of hydrogen bond acceptors, the count of hydrogen bond donors, and lipophilicity (LogP) values, were evaluated based on Lipinski's rule of five.

2.6. Molecular dynamics simulation.

Validation of the docking results was done using MD simulations for both the reference drug and the identified hit candidate. Input files for the protein-ligand complexes were prepared using the CHARMM-GUI platform (https://www.charmm-gui.org/), incorporating the protein in PDB format and the ligand in MOL2 format. A 10 Å rectangular simulation box was set to ensure accurate molecular interaction modeling. The system was solvated by adding water molecules and ions (0.15 M K+ and Cl-) to neutralize its charge. Parameter files were generated using the AMBER force field (GAFF2), which is compatible with the AMBER ff19SB protein force field, as demonstrated by Owolabi *et al*. [36]. The complexes underwent 100,000 steps of energy minimization, followed by a 5-nanosecond (ns) equilibration and a 100-ns production run. The equilibration was conducted under an NVT ensemble, while the production phase used an NPT ensemble, maintaining a stable temperature of 310.15 K. Trajectory analysis was performed using the CPPTRAJ module, and the binding interactions and free energies (ΔGbind) of the protein-ligand complexes were assessed using the Molecular Mechanics Generalized-Boltzmann Surface Area (MMGBSA) method.

3. Results and Discussion

3.1. Orbital energies and reactivity descriptors.

Various reactivity descriptors were calculated using 6-31+G* as a basis set via the density functional theory method. The descriptors considered were frontier molecular orbitals (highest occupied molecular orbital and lowest unoccupied molecular orbital energies), dipole moment, energy gap, weight, polar surface area (PSA), ovality, lipophilicity (LogP), polarizability, hydrogen bond donor, and hydrogen bond acceptor. According to Oyeneyin *et al*., frontier molecular orbitals have been observed to be involved in any chemical processes, and this has been engaged in forecasting any molecule's reactivity [37]. HOMO energy reveals the capacity of any molecule to donate electron while LUMO energy exposes the electron accepting capacity of any compound; thus, -7.34 eV, -5.38 eV, -5.50 eV, -6.91 eV, -7.02 eV, -6.09 eV, -6.91 eV, and -7.09 eVthe calculated HOMO energy while -0.38 electron volt, -2.08 electron volt, -2.04 eV, -1.30 eV, -0.02 eV, 0.05 eV, 0.08 eV, and 0.32 eVfor the calculated LUMO energy for compound 1-8. The differences between the calculated HOMO and LUMO energies, which depict the energy gap, revealed the stability and reactivity of any compound, and the calculated energy gap for the studied compounds was 6.96 eV, 3.30 eV, 3.46 eV, 5.61 eV, 7.00 eV, 6.14 eV, 6.99 eV, and 7.41 eV. According to Oyeneyin *et al*. [37], compounds with low calculated energy gaps depict higher reactivity than compounds with higher calculated energy gaps.

As shown in Table 2, the calculated HOMO energy for these optimized compounds ranges from -5.38 eV to -7.34 eV, while the calculated LUMO energy ranges from 0.32 eV to -2.08 eV. This depicts that compound 2 (-5.38 eV) readily donates more electrons than other optimized compounds, while compound 1 (-7.34 eV) donates the least electrons among the studied compounds. The values shown for the calculated HOMO energy for the optimized compounds revealed that the capacity of all the studied compounds to donate electrons was closer to one another. Meanwhile, the same trend observed in HOMO energy was observed in

LUMO energy; compound 2 (-2.08 eV) accepts electrons from the compound with the ability to donate them more readily than other optimized compounds. However, compound 8 (0.32 eV) showed the least ability to accept electrons from neighboring compounds. More so, the calculated energy gap for the studied compounds was observed to follow a similar trend when compared to the LUMO energy for the optimized compounds. Compound 2 (3.30 eV) depicts higher reactivity than other studied compounds, while compound 8 (7.41 eV) proved to be more stable than other studied compounds. More so, the energy gap is crucial for determining the molecule's stability and reactivity, influencing its biological function. A wider energy gap generally indicates greater stability and lower reactivity, while a smaller gap suggests the opposite. Therefore, compound 2 was found to be reactive than the other studied compounds.

Moreover, according to Oyebamiji *et al*. [38], the molecular weight (MW) for any molecular compound is expected to be less than or equal to 500 amu (≤500 amu); thus, all the studied compounds were observed to possess the potential ability to act as a drug-like agent. Also, the calculated hydrogen bond donor (HBD) and hydrogen bond acceptor (HBA) for compounds 1 to 8 were within the acceptable range (HBD: ≤5 and HBA≤10), indicating the probable capacity of compounds 1 to 8 to exhibit drug-like ability.

Table 2. Calculated 3-D Properties of the studied/optimized compounds.

	E_H (eV)	E_L (eV)	Energy gap (eV)	Dipole moment (Debye)	Weight (Amu)	PSA (Å)	Ovality	Log P	Pol	HBD	HBA
1	-7.34	-0.38	6.96	4.96	134.131	51.933	1.21	-1.10	50.34	2	3
2	-5.38	-2.08	3.30	2.33	207.276	7.408	1.32	4.44	59.21	0	1
3	-5.50	-2.04	3.46	3.53	154.209	31.040	1.27	1.94	54.59	1	2
4	-6.91	-1.30	5.61	4.87	390.564	37.713	1.72	7.46	76.60	0	2
5	-7.02	-0.02	7.00	3.99	158.241	20.089	1.32	2.84	54.94	0	1
6	-6.09	0.05	6.14	4.26	280.452	35.189	1.62	5.97	67.83	1	1
7	-6.91	0.08	6.99	4.40	256.430	35.189	1.62	5.77	65.52	1	1
8	-7.09	0.32	7.41	4.64	284.484	34.273	1.67	6.61	68.37	1	1

PSA- polar surface area; Log P-lipophilicity; pol-polarizability; HBD-hydrogen bond donor; HBA-hydrogen bond acceptor.

3.2. Induced fit molecular docking at the binding site of 2G56.

All the compounds with potential drug-like ability were subjected to docking studies, and the predicted outputs were compared to the output of the reference compound (Metformin). The output (Scoring) for the docked compounds was presented in Table 3, while the nonbonding interactions observed between the docked complexes were shown in Table 4 and Figure 1. The calculated binding affinity and the predicted nonbonding interactions involved in the studied complexes were -7.10786152 kcal/mol (PRO 101 H-donor; TYR 224 H-acceptor; PHE 218 H-acceptor; PRO 101 pi-H) for Compound 1, -7.13188314 kcal/mol (LEU 285 H-acceptor; LYS 74 pi-cation) for Compound 2, -7.96747208 kcal/mol (ASN 841 H-donor; ARG 765 H-acceptor; ARG 765 H-acceptor) for Compound 3, -6.99422932 kcal/mol (ASN 252 H-donor; HIS 442 H-donor) for Compound 4, -7.04297304 kcal/mol (ASN 252 H-acceptor; LEU 285 H-acceptor; LYS 74 pi-cation) for Compound 5, -6.65279293 kcal/mol (LYS 74 H-acceptor; LYS 74 pi-cation) for Compound 6, -6.92597628 kcal/mol (GLU 133 H-donor; MET 870 H-donor; GLU 880 H-donor; THR 878 H-acceptor) for Compound 7, -7.02212143 kcal/mol (CYS 819 H-donor) for Compound 8, -7.71405029 kcal/mol (ARG 765 H-acceptor; LYS 558 H-acceptor; PRO 760 pi-H) for Compound 9, -6.70089579 kcal/mol (ARG 368 H-acceptor; ARG 49 H-acceptor) for Compound 10.

According to reports from several literatures, biological and biochemical strength of ligand(s) may show the inhibiting ability against receptor and it may not also disclose it [39, 40].

Table 3. Calculated scoring and amino acid residue.

	Binding affinity (kcal/mol)	Amino Acid residues
1	-7.10	PRO 101 H-donor TYR 224 H-acceptor PHE 218 H-acceptor PRO 101 pi-H
2	-7.13	LEU 285 H-acceptor LYS 74 pi-cation
3	-7.96	ASN 841 H-donor ARG 765 H-acceptor ARG 765 H-acceptor
4	-6.99	ASN 252 H-donor HIS 442 H-donor
5	-7.04	ASN 252 H-acceptor LEU 285 H-acceptor LYS 74 pi-cation
6	-6.65	LYS 74 H-acceptor LYS 74 pi-cation
7	-6.92	GLU 133 H-donor MET 870 H-donor GLU 880 H-donor THR 878 H-acceptor
8	-7.02	CYS 819 H-donor
9	-7.71	ARG 765 H-acceptor LYS 558 H-acceptor PRO 760 pi-H
10	-6.70	ARG 368 H-acceptor ARG 49 H-acceptor
Ref	-5.30	GLY 909 Carbon-Hydrogen Bond GLN 800 Conventional Hydrogen Bond ASN 805 Conventional Hydrogen Bond GLU 924 Attractive Charge GLU 809 Salt Bridge

*Ref: Metformin

Note: *tables are original and non-published or taken from open-access sources*

Table 4. Ligand-receptor nonbonding Interaction diagrams of compounds 1 to 10 with the amino acid residues of 2G56.

Compounds	Ligand-receptor nonbonding interaction
1	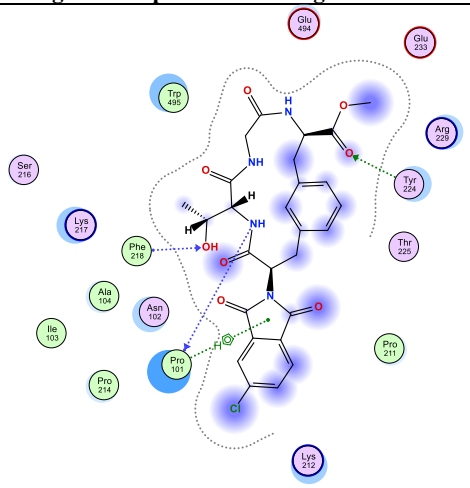

Compounds	Ligand-receptor nonbonding interaction
2	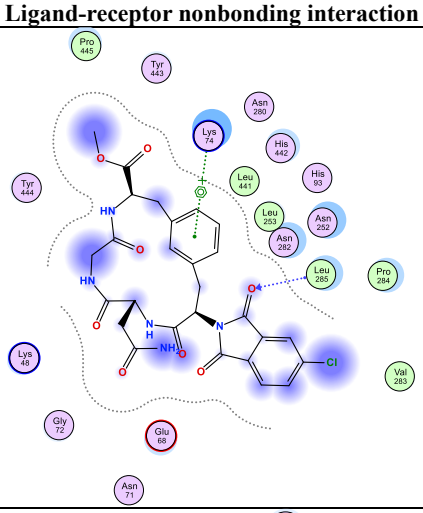
3	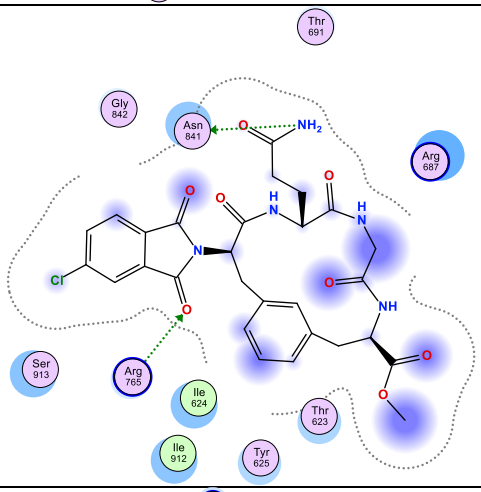
4	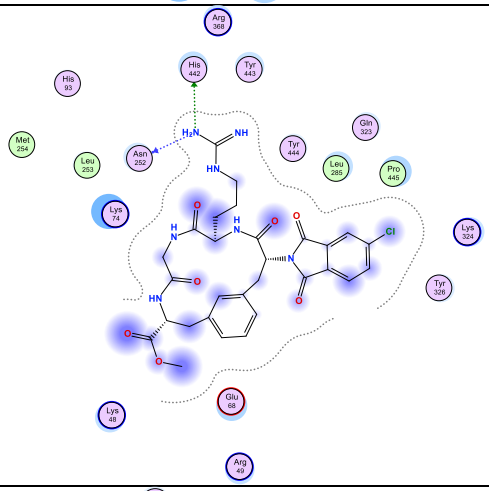
5	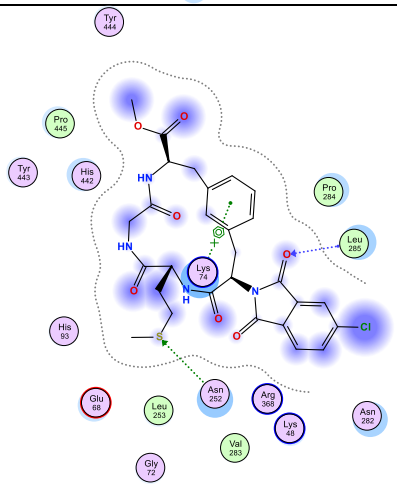

Compounds	Ligand-receptor nonbonding interaction
6	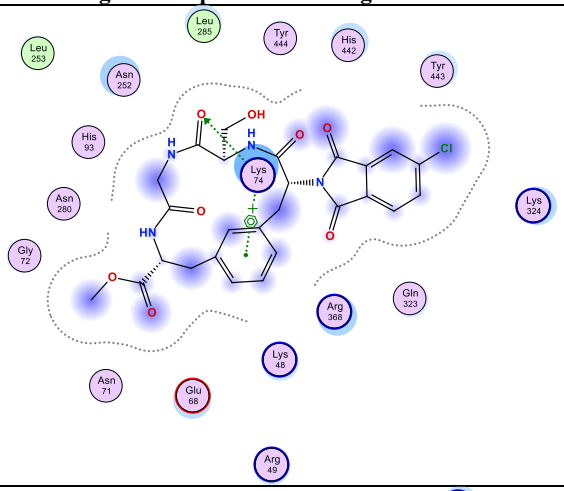
7	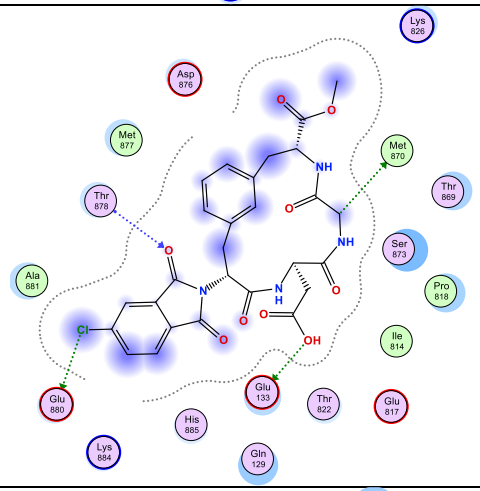
8	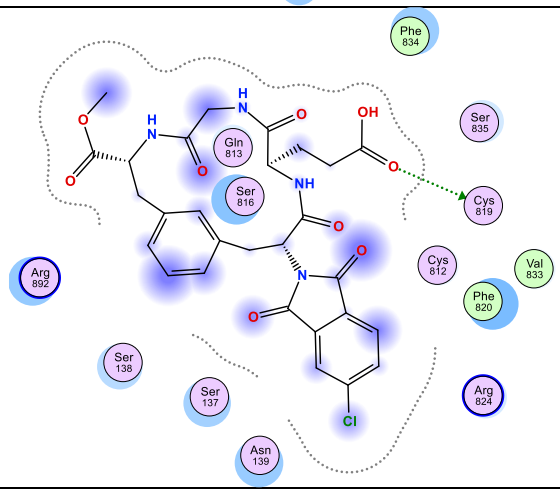
9	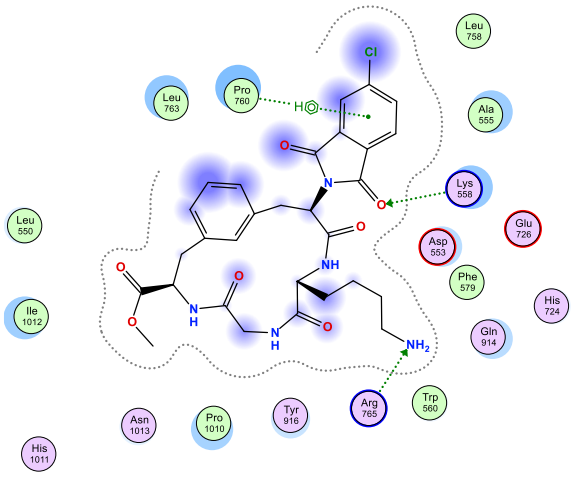

Compounds	Ligand-receptor nonbonding interaction
10	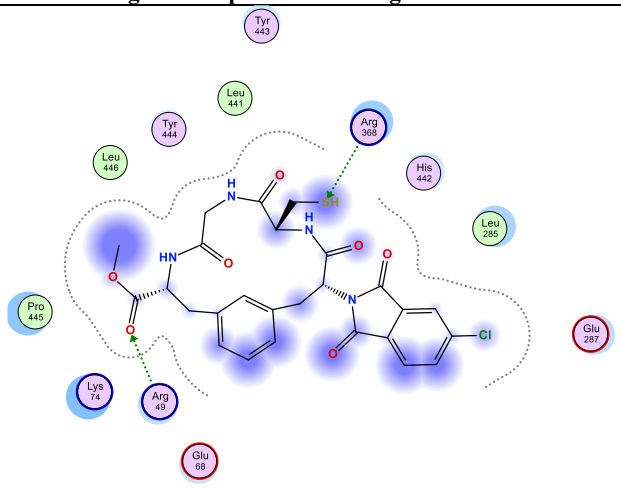

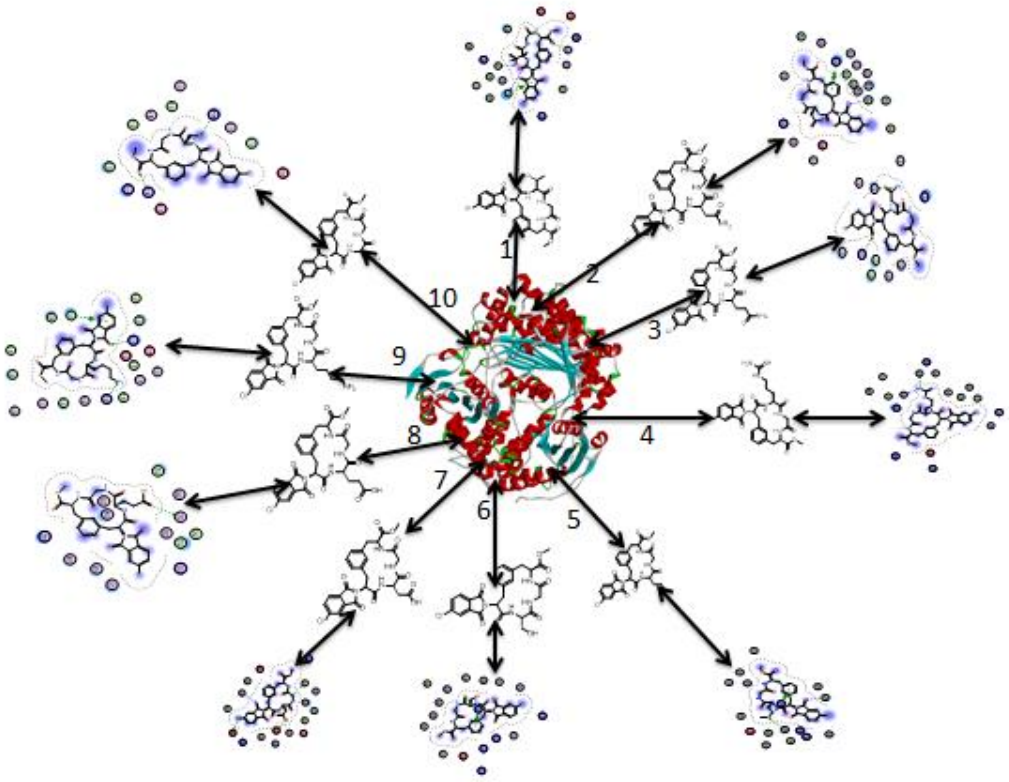

Figure 1. Pictorial representation of the docked studied complexes.

However, Latona *et al*. reported that inhibition of receptor by ligand exposes the type of nonbonding interaction that occurred between the studied complexes as well as coordination of the atom(s) in the ligands [41] and compound with lowest binding affinity is considered to be have greatest strength to inhibit receptor [42-55]; therefore, methyl (3S,9S,12S)-9-(3-amino-3-oxopropyl)-12-(5-chloro-1,3-dioxoisoindolin-2-yl)-5,8,11-trioxo-4,7,10-triaza-1(1,3)-benzenacyclotridecaphane-3-carboxylate (Compound 3) proved to possess the ability to regulate the biochemical and biological activities of Human insulin-degrading enzyme (PDB ID: 2g56) (Table 3). The unique inhibiting activity of compound 3 could be attributed to the release of electron from the amine group of methyl (3S,9S,12S)-9-(3-amino-3-oxopropyl)-12-(5-chloro-1,3-dioxoisoindolin-2-yl)-5,8,11-trioxo-4,7,10-triaza-1(1,3)-benzenacyclotridecaphane-3-carboxylate (Compound 3) to ASN841 as well as the receiver of

electron by carbonyl group of compound 3 from ARG 765. Also, the point of interaction of methyl (3S,9S,12S)-9-(3-amino-3-oxopropyl)-12-(5-chloro-1,3-dioxoisoindolin-2-yl)-5,8,11-trioxo-4,7,10-triaza-1(1,3)-benzenacyclotridecaphane-3-carboxylate (Compound 3) with ARG 765 and ASN841 revealed that the complex formed was stable with a high level of efficiency and selectivity (Table 3 and Figure 1). More so, all the studied compounds proved to be active than the studied referenced compound.

3.3. Predicted pharmacokinetics.

In this work, various factors were considered to investigate the pharmacokinetic study of the selected compounds (compound 3 and the reference compound). As shown in Table 5, blood-brain barrier, human intestinal absorption, Caco-2 permeability, P-glycoprotein Substrate, P-glycoprotein inhibitor, and Renal Organic Cation Transporter were examined for the absorption ability of the selected compounds. It was observed that the calculated probabilities of the selected compounds were fairly correlated, and the results were also similar except for P-glycoprotein Substrate for compound 3, which was observed to be a substrate while it was a non-substrate for the reference compound. This is proof that methyl (3S,9S,12S)-9-(3-amino-3-oxopropyl)-12-(5-chloro-1,3-dioxoisoindolin-2-yl)-5,8,11-trioxo-4,7,10-triaza-1(1,3)-benzenacyclotridecaphane-3-carboxylate (Compound 3) has a fair ability to be absorbed in the human body system. Also, the results and probabilities calculated for distribution, metabolism, and toxicity for the selected compounds depict the capacity of the lead compound to act as a potential drug agent. More so, the selected compound was predicted not to be biodegradable and goes in line with the reference compound used in this work.

Table 5. ADMET predicted profile --- classification and regression.

Model	**Result**		**Probability**	
Absorption				
	Compound 3	Metformin	Compound 3	Metformin
Blood-Brain Barrier	BBB+	BBB+	0.6788	0.5868
Human Intestinal Absorption	HIA+	HIA+	0.9514	0.9156
Caco-2 Permeability	Caco2-	Caco2-	0.7177	0.8958
P-glycoprotein Substrate	Substrate	Non-substrate	0.7412	0.6643
P-glycoprotein Inhibitor	Non-inhibitor	Non-inhibitor	0.7761	0.9613
	Non-inhibitor	Non-inhibitor	0.8420	0.8892
Renal Organic Cation Transporter	Non-inhibitor	Non-inhibitor	0.8117	0.7518
Distribution				
Subcellular localization	Lysosome	Lysosome	0.3876	0.7916
Metabolism				
CYP450 2C9 Substrate	Non-substrate	Non-substrate	0.8402	0.7929
CYP450 2D6 Substrate	Non-substrate	Non-substrate	0.8290	0.7325
CYP450 3A4 Substrate	Substrate	Non-substrate	0.6375	0.6906
CYP450 1A2 Inhibitor	Non-inhibitor	Non-inhibitor	0.7666	0.9046
CYP450 2C9 Inhibitor	Non-inhibitor	Non-inhibitor	0.5229	0.9159
CYP450 2D6 Inhibitor	Non-inhibitor	Non-inhibitor	0.8169	0.9231
CYP450 2C19 Inhibitor	Non-inhibitor	Non-inhibitor	0.5000	0.9130
CYP450 3A4 Inhibitor	Inhibitor	Non-inhibitor	0.8467	0.9506
CYP Inhibitory Promiscuity	Low CYP Inhibitory Promiscuity	Low CYP Inhibitory Promiscuity	0.6297	0.9763
Toxicity				
Human Ether-a-go-go-Related Gene Inhibition	Weak inhibitor	Weak inhibitor	0.9750	0.9807
	Inhibitor	Non-inhibitor	0.6799	0.9274
AMES Toxicity	Non-AMES toxic	Non-AMES toxic	0.7689	0.7367
Carcinogens	Non-carcinogens	Non-carcinogens	0.8868	0.6691
Fish Toxicity	High FHMT	Low FHMT	0.9809	0.8761
Tetrahymena Pyriformis Toxicity	High TPT	Low TPT	0.9869	0.9005

Honey Bee Toxicity	Low HBT	Low HBT	0.8617	0.5816
Biodegradation	Not ready biodegradable	Not ready biodegradable	0.9971	0.9380
Acute Oral Toxicity	III	III	0.5761	0.7817
Carcinogenicity (Three-class)	Non-required	Non-required	0.5715	0.6357
ADMET Predicted Profile --- Regression				
Model	Value		Unit	
Absorption				
Aqueous solubility	-3.6562	-0.9180	LogS	LogS
Caco-2 Permeability	-0.0937	0.2041	LogPapp, cm/s	LogPapp, cm/s
Toxicity				
Rat Acute Toxicity	2.7023	1.7407	LD50, mol/kg	LD50, mol/kg
Fish Toxicity	1.1815	2.2781	pLC50, mg/L	pLC50, mg/L
Tetrahymena Pyriformis Toxicity	0.5599	-0.6614	pIGC50, ug/L	pIGC50, ug/L

3.4. Molecular dynamic simulation analysis.

In this study, various binding free energies were calculated, along with root mean square deviation (RMSD) and root mean square fluctuation (RMSF) analyses, to evaluate the molecular dynamics (MD) simulation outcomes of methyl (3S,9S,12S)-9-(3-amino-3-oxopropyl)-12-(5-chloro-1,3-dioxoisoindolin-2-yl)-5,8,11-trioxo-4,7,10-triaza-1(1,3)-benzenacyclotridecaphane-3-carboxylate (Compound 3), as well as a reference compound, in complex with human insulin-degrading enzyme (IDE; PDB ID: 2G56). As shown in Table 6, the gas-phase binding energy (ΔG_{gas}) was more favorable for the reference compound (−129.75 kcal/mol) compared to Compound 3 (−125.16 kcal/mol), indicating stronger gas-phase interactions for the reference.

Table 6. Calculated free energies for compound **3** and reference compound against 2g56.

Compound	ΔG_{gas} (kcal/mol)	ΔG_{solv} (kcal/mol)	MMGBSA (kcal/mol)
Compd 3-2g56	-84.45	51.95	-32.49
Ref-2g56	-915.01	978.73	63.72

However, in the solvated phase, Compound 3 exhibited a more favorable solvation energy (ΔG_{solv} = 92.67 kcal/mol) compared to the reference compound (ΔG_{solv} = 97.83 kcal/mol), suggesting better stability and solvation behavior in a physiological environment.

The total binding energy, which combines gas-phase and solvation effects, indicated that Compound 3 had the most favorable overall interaction energy with IDE, with a calculated value of −32.49 kcal/mol, compared to −31.92 kcal/mol for the reference compound. According to Abdul-Hammed *et al*. [56], compounds with lower (more negative) binding energies generally exhibit stronger inhibitory potential. Therefore, Compound 3 demonstrates superior inhibitory capacity against human insulin-degrading enzyme.

The structural stability of both complexes during the simulation was evaluated using RMSD and RMSF analyses, as depicted in Figures 2 and 3. Compound 3 maintained a more stable binding conformation over the simulation period, with a lower RMSD value compared to the reference compound, indicating less deviation from its initial conformation. Furthermore, RMSF analysis revealed reduced atomic fluctuations for Compound 3, especially within the active site region, suggesting stronger and more stable interactions with IDE.

Additionally, the interaction profile of Compound 3 showed more consistent and extensive contacts with the enzyme's key residues, further supporting its enhanced binding affinity. The improved performance of Compound 3 can be attributed to its favorable structural conformation and interaction energy, which may be influenced by the electronic effects of its

substituents. Therefore, the binding free energy calculations, supported by RMSD and RMSF analyses, strongly indicate that Compound 3 is a promising candidate for further development as a potential inhibitor of human insulin-degrading enzyme.

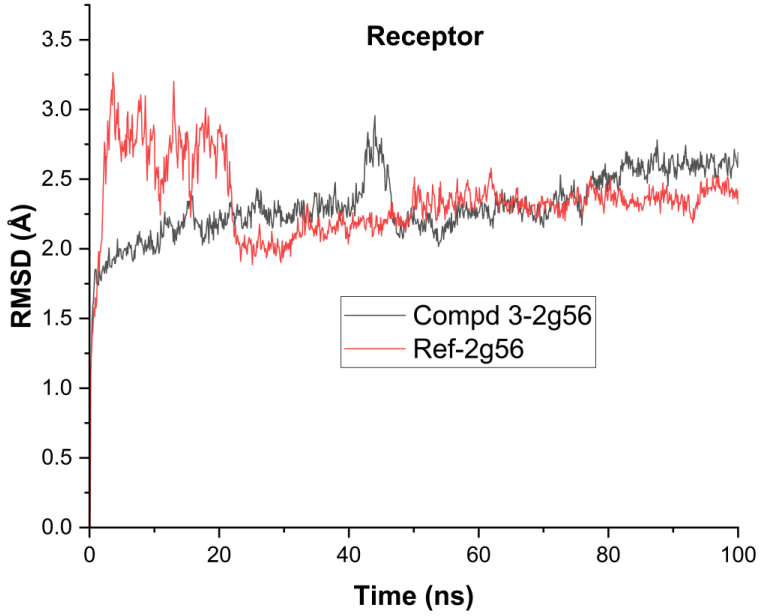

Figure 2. Predicted RMSD for compound **3** and reference compound against 2g56.

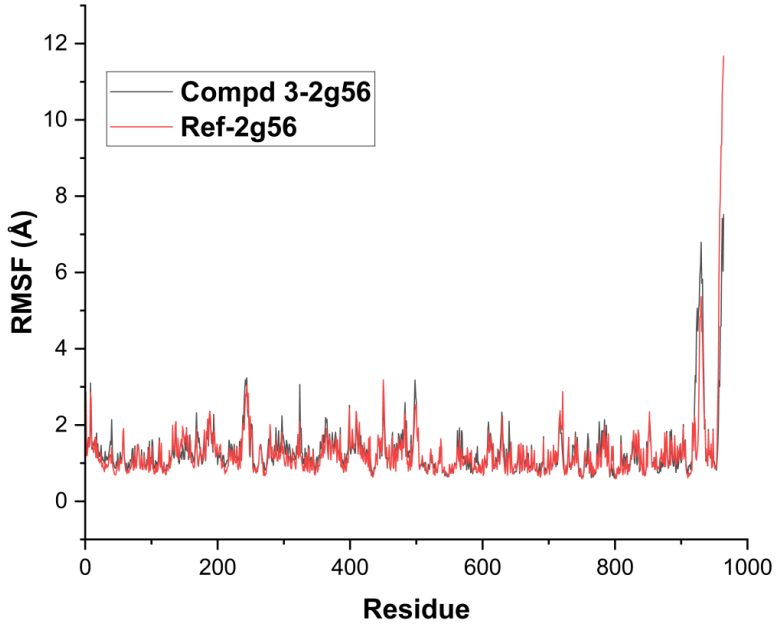

Figure 3. Predicted RMSF for compound 3 and reference compound against 2g56.

4. Conclusions

The modified cyclic tetra-amino acid-based compounds against human insulin-degrading enzyme were investigated using an *in silico* method. The 3-dimensional descriptors were examined, and human insulin-degrading enzyme inhibitor activities of modified cyclic tetra-amino acid-based compounds were examined. More so, the addition of propionamide to the modified cyclic tetra-amino acid-based compounds improved a comprehensive improvement in the hydrogen bond strength with ARG 765 and ASN841 located in the binding site of human insulin-degrading enzyme (2g56). Moreover, the molecular docking of methyl

(3S,9S,12S)-9-(3-amino-3-oxopropyl)-12-(5-chloro-1,3-dioxoisoindolin-2-yl)-5,8,11-trioxo-4,7,10-triaza-1(1,3)-benzenacyclotridecaphane-3-carboxylate and human insulin-degrading enzyme (2g56) showed a good binding inclination with calculated binding affinity value of -7.96747208 kcal mol^{-1}, demonstrating that it has a greater propensity to inhibit the enzyme than other compounds under study. Additionally, investigating their capabilities as inhibitors of the human insulin-degrading enzyme, this research may aid in the thoughtful design and creation of an extensive collection of effective, modified cyclic tetra-amino acid derivatives for prospective therapeutic uses.

Author Contributions

Conceptualization, A.K.O. and C.O.A.; methodology, A.I.O.; software, S.A.A.; validation, S.O.A, S.A.A., and A.K.O.; formal analysis, A.K.O.; investigation, A.K.O.; resources, C.O.A.; data curation, A.I.O.; writing—original draft preparation, A.K.O.; writing—review and editing, A.K.O.; visualization, C.O.A.; supervision, C.O.A.; project administration, A.K.O.; funding acquisition, C.O.A. All authors have read and agreed to the published version of the manuscript.

Institutional Review Board Statement

Not applicable.

Informed Consent Statement

Not applicable.

Data Availability Statement

The data of this study are available from the corresponding author upon reasonable request.

Funding

This work was supported by TETfund. IBR/FUOYE/2019-2023/02.

Acknowledgments

We are grateful to the Department of Chemistry, Federal University, Oye-Ekiti, Ekiti State, for both experimental and computational resources and to Mrs E.T. Oyebamiji, Miss Priscilla F. Oyebamiji, and John O. Oyebamiji for the assistance in the course of this study.

Conflicts of Interest

The authors declare no conflict of interest.

References

1. Patience, O.O.; Estella, U.O.; Philip, F.U. Natural Products as Potential Sources of Antidiabetic Drugs. *Br. J. Pharm. Res.* **2014**, *4*, 2075-2095, https://doi.org/10.9734/BJPR/2014/8382.
2. Kerru, N.; Singh-Pillay, A.; Awolade, P.; Singh, P. Current anti-diabetic agents and their molecular targets: A review. *Eur. J. Med. Chem.* **2018**, *152*, 436-488, https://doi.org/10.1016/j.ejmech.2018.04.061.
3. Passakorn, T.; Rachanida, P.; Benjaporn, N.; Surat, L.; Panupong, P. Anti-diabetic compounds from *Uvaria dulcis* Dunal. *Heliyon* **2024**, *10*, e26962, https://doi.org/10.1016/j.heliyon.2024.e26962.

4. Heidarpour, M.; Mojarad, M.; MazaheriTehrani, S.; Kachuei, A.; Najimi, A.; Shafie, D.; Rezvania, H. Comparative Effectiveness of Antidiabetic Drugs as an Additional Therapy to Metformin in Women with Polycystic Ovary Syndrome: A Systematic Review of Metabolic Approaches. *Int. J. Endocrinol.* **2024**, *2024*, 9900213, https://doi.org/10.1155/2024/9900213.
5. Bidulka, P.; Lugo-Palacios, D.G.; Carroll, O.; O'Neill, S.; Adler, A.I.; Basu, A.; Silverwood, R.J.; Bartlett, J.W.; Nitsch, D.; Charlton, P.; Briggs, A.H.; Smeeth, L.; Douglas, I.J.; Khunti, K.; Grieve, R. Comparative effectiveness of second line oral antidiabetic treatments among people with type 2 diabetes mellitus: emulation of a target trial using routinely collected health data. *BMJ* **2024**, *385*, e077097, https://doi.org/10.1136/bmj-2023-077097.
6. Marcianò, G.; Vocca, C.; Casarella, A.; Gallelli, L.; Rania, V.; De Sarro, C.; Citraro, R.; Palleria, C.; Bianco, R.C.; Fera, I. The Prescription and Safety of Oral Antidiabetic Drugs in Outpatients with Type 2 Diabetes Mellitus: An Observational, Retrospective, Multicenter Study on the Role of Adherence in a Real-Life Primary Care Setting. *Diabetology* **2024**, *5*, 333-343, https://doi.org/10.3390/diabetology5030025.
7. Dahlén, A.D.; Dashi, G.; Maslov, I.; Attwood, M.M.; Jonsson, J.; Trukhan, V.; Schiöth, H.B. Trends in Antidiabetic Drug Discovery: FDA Approved Drugs, New Drugs in Clinical Trials and Global Sales. *Front. Pharmacol.* **2022**, *12*, 807548, https://doi.org/10.3389/fphar.2021.807548.
8. Ju, M.; Deng, T.; Jia, X.; Gong, M.; Li, Y.; Liu, F.; Yin, Y. The causal relationship between anti-diabetic drugs and gastrointestinal disorders: a drug-targeted mendelian randomization study. *Diabetol. Metab. Syndr.* **2024**, *16*, 141, https://doi.org/10.1186/s13098-024-01359-z.
9. Wronka, M.; Krzemińska, J.; Młynarska, E.; Rysz, J.; Franczyk, B. New Insights into the Use of Liraglutide—Impact on Cardiovascular Risk and Microvascular Outcomes. *Biomedicines* **2023**, *11*, 1159, https://doi.org/10.3390/biomedicines11041159.
10. Leissring, M.A.; González-Casimiro, C.M.; Merino, B.; Suire, C.N.; Perdomo, G. Targeting Insulin-Degrading Enzyme in Insulin Clearance. *Int. J. Mol. Sci.* **2021**, *22*, 2235, https://doi.org/10.3390/ijms22052235.
11. González-Casimiro, C.M.; Merino, B.; Casanueva-Álvarez, E.; Postigo-Casado, T.; Cámara-Torres, P.; Fernández-Díaz, C.M.; Leissring, M.A.; Cózar-Castellano, I.; Perdomo, G. Modulation of insulin sensitivity by insulin-degrading enzyme. *Biomedicines* **2021**, *9*, 86, https://doi.org/10.3390/biomedicines9010086.
12. Makarova, K.S.; Grishin, N.V. Thermolysin and mitochondrial processing peptidase: How far structure-functional convergence goes. *Protein Sci.* **1999**, *8*, 2537–2540, https://doi.org/10.1110/ps.8.11.2537.
13. Fernández-Gamba, A.; Leal, M.C.; Morelli, L.; Castano, E.M. Insulin-degrading enzyme: Structure-function relationship and its possible roles in health and disease. *Curr. Pharm. Des.* **2009**, *15*, 3644–3655, https://doi.org/10.2174/138161209789271799.
14. Chavda, V.P.; Solanki, H.K.; Davidson, M.; Apostolopoulos, V.; Bojarska, J. PeptideDrug Conjugates: A New Hope for Cancer Management. *Molecules* **2022**, *27*, 7232, https://doi.org/10.3390/molecules27217232.
15. Apostolopoulos, V.; Bojarska, J.; Chai, T.T.; Elnagdy, S.; Kaczmarek, K.; Matsoukas, J.; New, R.; Parang, K.; Lopez, O.P.; Parhiz, H.; Perera, C.O.; Pickholz, M.; Remko, M.; Saviano, M.; Skwarczynski, M.; Tang, Y.; Wolf, W.M.; Yoshiya, T.; Zabrocki, J.; Zielenkiewicz, P.; AlKhazindar, M.; Barriga, V.; Kelaidonis, K.; Sarasia, E.M.; Toth, I. A Global Review on Short Peptides: Frontiers and Perspectives. *Molecules* **2021**, *26*, 430, https://doi.org/10.3390/molecules26020430.
16. Apostolopoulos, V.; Bojarska, J.; Feehan, J.; Matsoukas, J.; Wolf, W. Smart therapies against global pandemics: A potential of short peptides. *Front. Pharmacol.* **2022**, *13*, 914467, https://doi.org/10.3389/fphar.2022.914467.
17. Apostolopoulos, V.; Bojarska, J.; Chai, T.T.; Feehan, J.; Kaczmarek, K.; Matsoukas, J.M.; Paredes-Lopez, O.; Saviano, M.; Skwarczynski, M.; Smith-Carpenter, J.; Venanzi, M.; Wolf, W.M.; Zielenkiewicz, P.; Ziora, Z.M. New Advances in Short Peptides: Looking Forward. *Molecules* **2022**, *27*, 3635, https://doi.org/10.3390/molecules27113635.
18. Bojarska, J.; Mieczkowski, A.; Ziora, Z.M.; Skwarczynski, M.; Toth, I.; Shalash, A.O.; Parang, K.; El-Mowafi, S.A.; Mohammed, E.H.M.; Elnagdy, S.; AlKhazindar, M.; Wolf, W.M. Cyclic Dipeptides: The Biological and Structural Landscape with Special Focus on the Anti-Cancer Proline-Based Scaffold. *Biomolecules* **2021**, *11*, 1515, https://doi.org/10.3390/biom11101515.
19. Costa, L.; Sousa, E.; Fernandes, C. Cyclic Peptides in Pipeline: What Future for These Great Molecules? *Pharmaceuticals* **2023**, *16*, 996, https://doi.org/10.3390/ph16070996.

20. Claro, B.; Bastos, M.; Garcia-Fandino, R. 4 - Design and applications of cyclic peptides. In Peptide Applications in Biomedicine, Biotechnology and Bioengineering, Koutsopoulos, S., Ed.; Woodhead Publishing: **2018**; pp. 87-129, https://doi.org/10.1016/B978-0-08-100736-5.00004-1.
21. Oyebamiji, A.K.; Akintayo, E.T.; Akintayo, C.O.; Aworinde, H.O.; Akintelu, S.A. Cyclic RGD-Containing Peptides: In Silico Exploration against BCL-X L. *Ukr. Biochem. J.* **2023**, *95*, 93-105, https://doi.org/10.15407/ubj95.02.093.
22. Chakraborty, S.; Tai, D.-F.; Lin, Y.-C.; Chiou, T.-W. Antitumor and Antimicrobial Activity of Some Cyclic Tetrapeptides and Tripeptides Derived from Marine Bacteria. *Mar. Drugs* **2015**, *13*, 3029-3045, https://doi.org/10.3390/md13053029.
23. Zasloff, M. Antimicrobial peptides of multicellular organisms. *Nature* **2002**, *415*, 389–395, https://doi.org/10.1038/415389a.
24. Becke, A.D. Density-functional thermochemistry. III. The role of exact exchange. *J. Chem. Phys.* **1993**, *98*, 5648-5652, https://doi.org/10.1063/1.464913.
25. Lee, C.; Yang, W.; Parr, R.G. Development of the Colle-Salvetti correlation-energy formula into a functional of the electron density. *Phys. Rev. B.* **1988**, *37*, 785-789, https://doi.org/10.1103/physrevb.37.785.
26. Shen, Y.; Joachimiak, A.; Rosner, M.R.; Tang, W.J. Structures of human insulin-degrading enzyme reveal a new substrate recognition mechanism. *Nature* **2006**, *443*, 870-874, https://doi.org/10.1038/nature05143.
27. Yonas, B.; Alfred, M.; Paballo, L.; Oyebamiji, A.K.; Adedapo, S.A.; Thierry, Y.F.; Lesetja, R.M. Molecular hybrid of 1,2,3-triazole and schiff base as potential antibacterial agents: DFT, molecular docking and ADME studies. *J. Mol. Struct.* **2023**, *1286*, 135617, https://doi.org/10.1038/s41598-024-57689-5.
28. Oyebamiji, A.K.; Akintelu, S.A.; Akande, I.O.; Aworinde, H.O.; Adepegba, O.A.; Akintayo, E.T.; Akintayo, C.O.; Semire, B.; Babalola, J.O. Dataset on biochemical inhibiting activities of selected phytochemicals in *Azadirachta indica L* as potential NS2B–NS3 proteases inhibitors. *Data Brief* **2023**, *48*, 109162, https://doi.org/10.1016/j.dib.2023.109162.
29. Oyebamiji, A.K.; Akintelu, S.A.; Odelade, K.A.; Adetuyi, B.; Akintayo, E.T.; Akintayo, C.O.; Semire, B. and Babalola, J.O. Electron Withdrawing Group Effect on Biological Activities of Pyrimidine Hybrids As Potential Anti-Matrix Metalloproteinase-7. *Quim. Nova.* **2023**, *46*, 791-797, http://dx.doi.org/10.21577/0100-4042.20230055.
30. Abraham, M.K.; Murtola, T.; Schulz, R.; Páll, S.; Smith, J.C.; Hess, B.; Lindahl, E. GROMACS: High performance molecular simulations through multi-level parallelism from laptops to supercomputers. *SoftwareX* **2015**, *1*, 19-25, https://doi.org/10.1016/J.SOFTX.2015.06.001.
31. Vanommeslaeghe, K.; Hatcher, E.; Acharya, C.; Kundu, S.; Zhong, S.; Shim, J.; Darian, E.; Guvench, O.; Lopes, P.; Vorobyov, I.; Mackerell, Jr. A.D. CHARMM general force field: A force field for drug-like molecules compatible with the CHARMM all-atom additive biological force fields. *J. Comput. Chem.* **2010**, *31*, 671-690, https://doi.org/10.1002/jcc.21367.
32. Zoete, V.; Cuendet, M.A.; Grosdidier, A.; Michielin, O. SwissParam: A fast force field generation tool for small organic molecules. *J. Comput. Chem.* **2011**, *32*, 2359-2368, https://doi.org/10.1002/jcc.21816.
33. Ulrich, E.; Lalith, P.; Max, L.B.; Tom, D.; Hsing, L.; Lee, G.P. A smooth particle mesh Ewald method. *J. Chem. Phys.* **1995**, *103*, 8577–8593, http://dx.doi.org/10.1063/1.470117.
34. Kumari, R.; Kumar, R. Open Source Drug Discovery Consortium, Andrew Lynn. *g_mmpbsa*—A GROMACS Tool for High-Throughput MM-PBSA Calculations. *J. Chem. Inf. Model.* **2014**, *54*, 1951–1962, https://doi.org/10.1021/ci500020m.
35. Daina, A.; Michielin, O.; Zoete, V. SwissADME: a free web tool to evaluate pharmacokinetics, drug-likeness and medicinal chemistry friendliness of small molecules. *Sci. Rep.* **2017**, *7*, e42717, https://doi.org/10.1038/srep42717.
36. Owolabi, A.O.; Akpor, O.B.; Ndako, J.A.; Owa, S.O.; Oluyori, A.P.; Oludipe, E.O.; Afolabi, S.O.; Asaleye, R.M. Antimicrobial potential of Hippocratea Indica Willd. Acetone Leaf fractions against Salmonella Typhi: an in vitro and in silico study. *Sci. Rep.* **2024**, *14*, 25222, https://doi.org/10.1038/s41598-024-75796-1.
37. Oyeneyin, O.E.; Moodley, R.; Mashaba, C.; Garnie, L.F.; Omoboyowa, D.A.; Rakodi, G.H.; Maphoru, M.V.; Balogun, M.O.; Hoppe, H.C.; Egan, T.J. In vitro antiplasmodium and antitrypanosomal activities, β-haematin formation inhibition, molecular docking and DFT computational studies of quinoline-urea-benzothiazole hybrids. *Heliyon* **2024**, *10*, e38434, https://doi.org/10.1016/j.heliyon.2024.e38434.

38. Oyebamiji, A.K.; Tolufashe, G.T.; Olubukola Monisola Oyawoye, O.M.; Oyedepo, T.A. and Semire, B. Biological Activity of Selected Compounds from *Annona muricata* Seed as Antibreast Cancer Agents: Theoretical Study. *J. Chem.* **2020**, *2020*, 6735232, https://doi.org/10.1155/2020/6735232.
39. Adeoye, M.D.; Olarinoye, E.F.; Oyebamiji, A.K.; Latona, D.F. Theoretical Evaluation of Potential Anti-Alanine Dehydrogenase Activities of Acetamide Derivatives. *Biointerface Res. Appl. Chem.* **2022**, *12*, 7469–7477, https://doi.org/10.33263/BRIAC126.74697477.
40. Oyebamiji, A.K.; Babalola, J.O.; Odelade, K.A.; Akintelu, S.A.; Nubi, O.A.; Aworinde, H.O.; Faboro, E.; Akintayo, E.T.; Semire, B. Potential inhibiting activities of phytochemicals in Scilla natalensis bulbs against schistosomiasis. *Eclética Química* **2023**, *48*, 54-80, https://doi.org/10.26850/1678-4618eqj.v48.3.2023.p54-80.
41. Latona, D.F.; Mutiu, O.A.; Adeoye, M.D.; Oyebamiji, A.K.; Akintelu, S.A.; Adedapo, A.S. In-Silico Investigation on Chloroquine Derivatives: A Potential Anti-COVID-19 Main Protease. *Biointerface Res. Appl. Chem*. **2022**, *12*, 8492–8501, https://doi.org/10.33263/BRIAC126.84928501.
42. Erazua, E.A.; Olaseinde, A.A.; Oyebamiji, A.K.; Oluwakemi, E.; Adekunle, D.; Olanrewaju, A.A.; Akinola, O.T.; Afolabi, S.O. Molecular docking and ADMET profiling of Carbazole-rhodanine hybrid as anticancer agent. *J. Phytomed. Ther.* **2024**, *23*, 1491-1515, https://doi.org/10.4314/jopat.v23i2.8.
43. Spassov, D.S. Binding Affinity Determination in Drug Design: Insights from Lock and Key, Induced Fit, Conformational Selection, and Inhibitor Trapping Models. *Int. J. Mol. Sci*. **2024**, *25*, 7124, https://doi.org/10.3390/ijms25137124.
44. Spassov, D.S.; Atanasova, M.; Doytchinova, I. Inhibitor Trapping in N-Myristoyltransferases as a Mechanism for Drug Potency. *Int. J. Mol. Sci.* **2023**, *24*, 11610, https://doi.org/10.3390/ijms241411610.
45. Oyebamiji, A.K.; Olujinmi, F.E.; Aworinde, H.O.; Oke, D.G.; Akintelu, S.A.; Akintayo, E.T.; Akintayo, C.O.; Babalola, J.O. Dataset on anti-human Insulin-Degrading Enzyme activities of Cyclic Tetra Peptides: Insight from Insilico Approach. *Data Brief.* **2024**, *55*, 110724. https://doi.org/10.1016/j.dib.2024.110724.
46. Spassov, D.S.; Atanasova, M.; Doytchinova, I. Inhibitor Trapping in Kinases. *Int. J. Mol. Sci.* **2024**, *25*, 3249, https://doi.org/10.3390/ijms25063249.
47. Singhal A.; Li B.T.; O'Reilly E.M. Targeting KRAS in cancer. *Nat. Med.* **2024**, *30*, 969–983, https://doi.org/10.1038/s41591-024-02903-0.
48. Pinheiro, P.S.M.; Franco, L.S.; Fraga, C.A.M. The Magic Methyl and Its Tricks in Drug Discovery and Development. *Pharmaceuticals* **2023**, *16*, 1157, https://doi.org/10.3390/ph16081157.
49. Akinola, O.T.; Oyebamiji, A.K.; Oke, D.G.; Adekunle, D.O.; Olanrewaju, A.A.; Akintelu, S.A. In silico analysis on binding action of beta-lactam drugs against TEM and SHV class A beta-lactamases from *Klebsiella pneumonia*. *Discov. Appl. Sci.* **2024**, *6*, 196, https://doi.org/10.1007/s42452-024-05783-8.
50. Ojha, A.A.; Srivastava, A.; Votapka, L.W.; Amaro, R.E. Selectivity and Ranking of Tight-Binding JAK-STAT Inhibitors Using Markovian Milestoning with Voronoi Tessellations. *J. Chem. Inf. Model.* **2023**, *63*, 2469–2482, https://doi.org/10.1021/acs.jcim.2c01589.
51. Rodríguez-Hernández, D.; Vijayan, K.; Zigweid, R.; Fenwick, M.K.; Sankaran, B.; Roobsoong, W.; Sattabongkot, J.; Glennon, E.K.; Myler, P.J.; Sunnerhagen, P. Identification of potent and selective N-myristoyltransferase inhibitors of Plasmodium vivax liver stage hypnozoites and schizonts. *Nat. Commun.* **2023**, *14*, 5408, https://doi.org/10.1038/s41467-023-41119-7.
52. Spassov, D.S.; Atanasova, M.; Doytchinova, I. A role of salt bridges in mediating drug potency: A lesson from the N-myristoyltransferase inhibitors. *Front. Mol. Biosci.* **2023**, *9*, 1066029, https://doi.org/10.3389/fmolb.2022.1066029.
53. McCullagh, M.; Zeczycki, T.N.; Kariyawasam, C.S.; Durie, C.L.; Halkidis, K.; Fitzkee, N.C.; Holt, J.M.; Fenton, A.W. What is allosteric regulation? Exploring the exceptions that prove the rule! *J. Biol. Chem.* **2024**, *300*, 105672, https://doi.org/10.1016/j.jbc.2024.105672.
54. Asibor, Y.E.; Oyebamiji, A.K.; Latona, D.F.; Semire, B. Computational screening of phytochemicals present in some Nigerian medicinal plants against sickle cell disease. *Sci. Rep.* **2024**, *14*, 26368, https://doi.org/10.1038/s41598-024-75078-w.
55. Zintle, M.; Mpho, C.; Eric, M.; Nwamadi, M.; Adeyemi, S.; Oyebamiji, A.K.; Adedapo, S.A.; Blassan, G.; Aderibigbe, B.A. Hybrid Molecules Containing Methotrexate, Vitamin D, and Platinum Derivatives: Synthesis, Characterization, *In Vitro* Cytotoxicity, *In Silico* ADME Docking, Molecular Docking and Dynamics. *Chem. Biodivers.* **2024**, *22*, e202400373, https://doi.org/10.1002/cbdv.202400373.
56. Abdul-Hammed, M.; Semire, B.; Adegboyega, S.A.; Oyebamiji, A.K.; and Olowolafe, T.A. Inhibition of Cyclooxygenase-2 and Thymidylate Synthase by Dietary Sphingomyelins: Insights from DFT and

Molecular Docking Studies. *Phys. Chem. Res*. **2020**, *8*, 296-310, https://doi.org/10.22036/PCR.2020.214026.1717.

Publisher's Note & Disclaimer